Mathematical Biosciences and Engineering

https://www.aimspress.com/journal/mbe

MBE, 23(6): 1596–1621.
DOI: 10.3934/mbe.2026058
Received: 16 January 2026
Revised: 23 March 2026
Accepted: 20 April 2026
Published: 28 April 2026

Research article

Stabilizing predator-prey interactions: the impact of supplementary food and anti-predator behavior

Aladeen Al Basheer*

Department of Basic Sciences, Al Hussein Technical University, King Abdullah II St 242, Amman 11831, Jordan

* **Correspondence:** Email: Aladeen.albasheer@htu.edu.jor; Tel: +962781252553.

Abstract: This study investigated a modified Holling-Tanner predator-prey model that incorporates supplementary food for predators and anti-predator behavior in prey. The model examined how these ecological mechanisms influence predator-prey dynamics and biological pest control. Local and global stability analyses were performed to determine the conditions that lead to predator persistence and pest eradication. Explicit parametric conditions were derived that guarantee global pest extinction, providing quantitative criteria for effective biological control. Bifurcation analysis revealed the presence of Hopf and saddle-node bifurcations, which identify critical parameter thresholds where the system transitions between stable equilibria, oscillatory dynamics, and collapse of coexistence states. The results showed that anti-predator behavior can stabilize population dynamics and suppress oscillatory behavior that would otherwise occur in the absence of prey defense mechanisms. A reaction-diffusion extension of the model was then considered to investigate spatial effects. Turing instability analysis demonstrated that the interaction between diffusion and anti-predator behavior can generate persistent spatial patterns, offering a mechanistic explanation for patchy predator distributions frequently observed in agricultural ecosystems. The analysis further indicated that the effectiveness of biological control depends on the balance between supplementary food quantity, predation pressure, and the strength of prey defense. Excessive food supplementation may reduce predator pressure on pests and weaken pest suppression. Numerical simulations supported the analytical results and illustrated parameter regimes that lead to system stabilization and successful pest management. The proposed framework provides theoretical guidance for designing predator-based biological control strategies that combine resource provisioning with natural behavioral responses.

Keywords: biological control; additional food; anti-predator; stability; Turing instability

1. Introduction

As an ecological management strategy, biological control serves as a sustainable approach to pest management, offering a sustainable substitute for chemical pesticides. It is particularly valuable because chemical controls, while widely practiced, are generally environmentally disruptive, unsustainable, and increasingly susceptible to pest resistance over time [1]. Biological control, on the other hand, involves introducing a predator species to enhance mortality among target pest populations [2–6]. However, the method is not without its problems. The predators do not usually eliminate the pests, and there could be collateral damage when the predators attack non-target organisms, causing unintended ecological impacts [7].

Because of these challenges, many studies have examined methods to enhance the effectiveness of natural predators in biological control programs. Experimental research has shown that providing supplementary food sources such as artificial honeydew or sugar sprays can increase predator abundance and improve their retention in agricultural habitats [8–11]. Field experiments in alfalfa and maize demonstrated that artificial honeydew can increase the numerical response of natural enemies and influence their spatial distribution, particularly for predators such as ladybird beetles [8, 10]. Similar studies reported that sugar applications enhance the activity of natural enemies and contribute to improved suppression of pests such as the fall armyworm [9]. The broader role of artificial food supplementation as a conservation biological control strategy has also been reviewed extensively [11].

Other studies have examined ecological and behavioral mechanisms that influence predator-prey interactions. In particular, predator interference has been shown to affect the establishment and effectiveness of generalist predators used in biological control programs [12]. In addition, experimental work demonstrates that prey nutritional quality can significantly influence predator feeding rates and trophic interactions [13]. Biological control strategies have also been explored in broader ecological contexts, including approaches used for the management of vertebrate pests [14], while sugar provisioning has been shown to increase the efficiency of parasitoids by improving their survival and reproductive performance [15].

Complementary theoretical and modeling studies have investigated ecological processes that modify predator-prey dynamics relevant to biological control. Mathematical models show that cannibalism in predator or prey populations can significantly alter system stability and long-term population dynamics [16, 17]. Other studies incorporate behavioral mechanisms such as predator-induced fear, demonstrating that fear effects can reduce prey reproduction and influence population stability [18, 19]. The ecological principles underlying these biological control strategies are well–established in foundational literature [7], while modern developments also emphasize the increasing role of environmentally safer pest management tools such as biopesticides [2]. One of these promising methods is the provision of supplemental or extra food to predators. There have been many field experiments that have tested this strategy, some of which have reported a significant reduction in pest populations when predators are given supplemental food. In [20] the authors found that supplying *Macrolophus pygmaeus*, a widely used natural enemy in biological control, with eggs of *Ephestia kuehniella* and pollen from *Typha latifolia* significantly increased the population density of *Macrolophus pygmaeus*. In [15] the authors found that the provision of sugar helped to augment the efficacy of parasitoids like *Binodoxys communis* in controlling soybean aphid populations.

Despite these promising outcomes, the precise factors that determine the success of supplemental

feeding remain elusive. Some studies, like [12], have highlighted complications such as predator interference or competition, which can undermine the efficiency of biological control agents. This has been observed across various predator types, including vertebrates and generalist predators. Additionally, the duration and frequency of supplemental feeding appear to have inconsistent effects, with complete pest eradication rarely achieved.

Mathematical models provides critical insights into predator-pest interactions, enabling identification of eradication parameters. The inclusion of supplementary feeding significantly alters system dynamics and management outcomes [21].

In previous studies [22–26], supplemental food has been shown to facilitate pest eradication across various predator-prey models, including Holling-type, Beddington-DeAngelis, and ratio-dependent models. However, the eradication process is gradual, occurring over an infinite time horizon rather than instantly. These models also reveal that certain ecological factors, such as pest refuges, can complicate outcomes. High levels of refuge availability can even lead to predator extinction despite the provision of supplemental food.

Although conventional theoretical approaches predominantly consider symmetrical predator responses, contemporary research has increasingly focused on asymmetric frameworks such as the Holling-Tanner model, which incorporates ratio-dependent predation dynamics. This model captures the complexities of predator-prey relationships more precisely, when incorporating supplemental food. Unlike symmetric models, the Holling-Tanner framework acknowledges the variability in predator responses to prey availability, offering insights into conditions that stabilize or destabilize the ecosystem. The work of [27] presented a modified Holling-Tanner formulation incorporating supplementary nutrition, demonstrating that resource augmentation can simultaneously enhance predator carrying capacity and reproductive rates. Prey species' evolved anti-predation strategies present significant challenges in modeling predator-prey interactions. In many cases, prey actively engage in defensive strategies, such as attacking juvenile predators, to reduce future predation risk [28–30]. While this behavior helps prey populations survive, it complicates biological control efforts because it weakens the predator's ability to reduce prey numbers effectively. In some situations, this can result in predator population decline and even lead to pest outbreaks [31, 32], as the prey population increases without sufficient predation pressure.

To mitigate these issues, supplemental feeding programs have been investigated as a potential strategy to enhance predator abundance in ecological systems and enhance their effectiveness in controlling pests. Supplementary food can help predators maintain their population size, even when prey numbers are low due to anti-predator behavior. Nevertheless, the efficacy of this approach critically depends on the nutritional composition, amount, and form of supplementary food. Studies show that providing the right kind of food can improve predator efficiency, leading to better pest control outcomes. For instance, some studies [33] has demonstrated that predators supplemented with high-quality food sources exhibit improved survival, reproduction, and predation rates, which in turn leads to more effective pest suppression. In [27], we investigated a Holling-Tanner predator-prey system with supplementary food supplied to the predator, establishing that resource augmentation can stabilize predator populations and enhance pest suppression. That analysis derived analytical conditions for equilibrium existence and local stability, including critical thresholds for pest extinction and predator persistence, and demonstrated that varying the quantity and quality of additional food can induce bifurcations driving transitions between stable equilibria and oscillatory

dynamics. While these findings provide quantitative guidance for optimizing predator-based biological control, the framework did not account for prey behavioral responses—a widespread ecological phenomenon that fundamentally alters predator-prey interactions.

In this paper, we examine how these two factors—supplementary food and anti-predator behavior—work together to affect predator-prey dynamics. We modify the classical Holling-Tanner model to include both, and then explore the conditions that lead to pest extinction, predator persistence, and system stability. Our analysis combines theory and simulation to support strategies for more reliable biological control.

This paper is structured as follows: Section 2 presents the mathematical model incorporating supplementary food and anti-predator behavior, followed by a comprehensive stability analysis of all biologically relevant equilibrium points. We establish the boundedness of solutions, derive conditions for local and global stability, and characterize the existence of limit cycles. Section 3 is devoted to bifurcation analysis, where we identify critical parameter thresholds for Hopf and saddle-node bifurcations, revealing how the system transitions between dynamical regimes. In Section 4, we extend the model to a reaction-diffusion framework and investigate Turing instability, deriving necessary and sufficient conditions for spatial pattern formation. Numerical simulations throughout validate our analytical findings and illustrate key dynamical behaviors. Finally, Section 5 discusses the ecological implications of our results for biological control strategies and outlines directions for future research.

2. Dynamical analysis of an additional food model incorporating anti-predator behavior

Building on the framework of [27], we extend the Holling-Tanner predator-prey framework by incorporating supplementary food for predators and adopting the standard Holling type-II response. We further enhance the model by introducing a prey defense mechanism that reduces predation. This leads to:

$$\left.\begin{aligned} u_t &= u(1-u) - \frac{suv}{\varpi + \alpha\beta + u}, \\ v_t &= \delta v\left(n + \frac{\beta}{\alpha\beta + u} - \frac{v}{\alpha\beta + u}\right) - quv \end{aligned}\right\}. \tag{2.1}$$

For readers interested in the full mathematical analysis of our model (Eq (2.10)), we recommend the detailed work in [27]. Here, we will focus on explaining what the different parameters actually mean in biological terms—you will find these clearly laid out in Table 1.

2.1. Equilibria and local stability

System (2.1) possesses four biologically meaningful equilibrium points:

- **Total extinction** $E_0 = (0, 0)$:
  Both predator and prey populations vanish from the ecosystem.
- **Prey-only equilibrium** $E_1 = (1, 0)$:
  Without predation pressure, prey species achieve their maximum equilibrium population size.

Table 1. Descriptions of variables and parameters present in system (2.1).

Symbol	Description
$u(t)$	Density of prey
$v(t)$	Density of predator
q	Strength of anti-predator effect
s	Rate of prey consumption by predator
ϖ	Prey impact on predator intake
α	Quality of supplemental food
β	Quantity of supplemental food
δ	Conversion efficiency of prey into predator growth
n	Baseline predator growth rate

- **Predator-persistence equilibrium** $E_2 = (0, n\alpha\beta + \beta)$:
  A critical case where predators maintain themselves through alternative food sources ($\alpha > 0$) despite prey extinction.
- **Coexistence equilibrium** $E^* = (u^*, v^*)$:
  The interior equilibrium where both species coexist, yielded by solving:

$$f(u, v) = (1 - u) - \left(\frac{sv}{\varpi + \alpha\beta + u}\right) = 0, \tag{2.2}$$

$$g(u, v) = n + \frac{\beta}{\alpha\beta + u} - \frac{v}{\alpha\beta + u} - \frac{q}{\delta}u = 0. \tag{2.3}$$

From equation Eq (2.2), we have

$$\frac{[(1 - u)(\varpi + \alpha\beta + u)]}{s} = v, \tag{2.4}$$

and from Eq (2.3), we have:

$$\left(n + \frac{\beta}{\alpha\beta + u} - \frac{q}{\delta}u\right)(\alpha\beta + u) = v, \tag{2.5}$$

$$\beta + \left(n - \frac{q}{\delta}u\right)(\alpha\beta + u) = v. \tag{2.6}$$

Substituting Eq (2.5) in Eq (2.4), we have

$$\frac{[(1 - u)(\varpi + \alpha\beta + u)]}{s} = \left(n + \tfrac{\beta}{\alpha\beta+u} - \tfrac{q}{\delta}u\right)(\alpha\beta + u),$$

which gives us

$$\tfrac{1}{s}(1 - u)(\varpi + \alpha\beta + u) - \left(n + \tfrac{\beta}{\alpha\beta+u} - \tfrac{q}{\delta}u\right)(\alpha\beta + u) = 0,$$
$$(\delta - qs)u^2 + (\varpi\delta - \delta + ns\delta + \alpha\beta\delta - qs\alpha\beta)u + \delta(s\beta - \varpi - \alpha\beta + ns\alpha\beta) = 0.$$

We use the following representations for the sake of simplicity:

$A = (\delta - qs)$, $B = (\varpi\delta - \delta + ns\delta + \alpha\beta\delta - qs\alpha\beta)$, and $C = \delta(s\beta - \varpi - \alpha\beta + ns\alpha\beta)$. Then we have three different cases:

1) A positive discriminant, $B^2 - 4AC > 0$, guarantees two real and unequal roots.

$$u_1^* = \frac{-B + \sqrt{B^2 - 4AC}}{2A}, \qquad v_1^* = \beta + \left(n - \frac{q}{\delta}u_1^*\right)(\alpha\beta + u_1^*),$$
$$u_2^* = \frac{-B - \sqrt{B^2 - 4AC}}{2A}, \qquad v_2^* = \beta + \left(n - \frac{q}{\delta}u_2^*\right)(\alpha\beta + u_2^*).$$

2) Provided that $B^2 = 4AC$ and $\frac{-B}{2A} > 0$, the analysis reveals that two equilibrium positions (u_1^*, v_1^*) and (u_2^*, v_2^*) meet at a single point, referred to as the instantaneous equilibrium $\bar{E}(\bar{u}, \bar{v})$, defined as follows:

$$\bar{u} = \frac{-(\varpi\delta - \delta + ns\delta + \alpha\beta\delta - qs\alpha\beta)}{2(\delta - qs)}, \qquad \bar{v} = \beta + \left(n - \frac{q}{\delta}\bar{u}\right)(\alpha\beta + \bar{u}).$$

3) When $A = 0$ (i.e., $\delta = qs$), $B \neq 0$, and $\frac{-C}{B} > 0$, there exists a single interior equilibrium point $\widehat{E}(\widehat{u}, \widehat{v})$ given by:

$$\widehat{u} = \frac{\varpi\delta + \alpha\beta\delta - s\beta\delta(n\alpha + 1)}{-\delta + \varpi\delta + ns\delta + \alpha\beta\delta - qs\alpha\beta}, \qquad \widehat{v} = \beta + \left(n - \frac{q}{\delta}\widehat{u}\right)(\alpha\beta + \widehat{u}).$$

Let $E(u^*, v^*)$ be the interior equilibrium of system (2.1). To compute the Jacobian matrix at this equilibrium, substitute u^* and v^* into the Jacobian matrix J.

$$J = \begin{pmatrix} u^*\left(-1 + \frac{sv^*}{(\varpi+\alpha\beta+u^*)^2}\right) + f(u^*, v^*) & -\frac{su^*}{\varpi+\alpha\beta+u^*} \\ \delta v^*\left(\frac{v^*-\beta}{(\alpha\beta+u^*)^2} - \frac{q}{\delta}\right) & \frac{-\delta v^*}{\alpha\beta+u^*} + \delta g(u^*, v^*) \end{pmatrix}.$$

We calculate the trace and determinant of J at each equilibrium and apply common linear stability conditions.

Theorem 2.1 (Stability analysis of equilibrium points)**.** *The system has the following stability properties at its equilibrium points:*

1) The origin $E_0 = (0, 0)$ is always unstable.
2) The axial equilibrium point $E_1 = (1, 0)$ is stable if $\delta\left(n + \frac{\beta}{\alpha\beta+1}\right) < q$ and saddle if $\delta\left(n + \frac{\beta}{\alpha\beta+1}\right) > q$.
3) The axial equilibrium point $E_2 = (0, n\alpha\beta + \beta)$ is
- *locally asymptotically stable if $\varpi < s(\alpha\beta + \beta) - \alpha\beta$ and $C > 0$,*
- *a saddle if $C < 0$, in which case at least one interior equilibrium exists.*

4) The interior equilibrium point (u^*, v^*) is stable when both of the following conditions are satisfied:

$$s < \left(u^* + \frac{\delta v^*}{\alpha\beta + u^*}\right)\left(\frac{(\varpi + \alpha\beta + u^*)^2}{u^* v^*}\right), \tag{2.7}$$
$$s < \frac{\delta(\varpi + \alpha\beta + u^*)^2(\alpha\beta + u^*)}{Q(u^*)}, \tag{2.8}$$

where $Q(u^*)$ is the polynomial

$$qu^{*3} + (3q\alpha\beta + q\varpi)u^{*2} + \beta(3q\alpha^2\beta + \delta + 2q\varpi\alpha)u^* + \beta(q\alpha^3\beta^2 + q\varpi\alpha^2\beta + \delta\alpha\beta + \varpi\delta) - \varpi\delta v^*.$$

Proof. The system described by Eq (2.1) admits several steady states, which are outlined below:

1) Consider the trivial equilibrium point $E_0 = (0, 0)$. To analyze its local behavior, we compute the Jacobian matrix evaluated at E_0, denoted by J_{E_0}, which is given by:

$$J_{E_0} = \begin{pmatrix} 1 & 0 \\ 0 & \delta\left(n + \frac{1}{\alpha}\right) \end{pmatrix}.$$

Since both eigenvalues at E_0 are positive, the origin behaves as an unstable node. This indicates that any small disturbance around E_0 will cause the system to move away from this point over time.

2) Consider the axial equilibrium point $E_1 = (1, 0)$. To examine its local behavior, we compute the Jacobian matrix evaluated at this point, denoted by J_{E_1}.

$$J_{E_1} = \begin{pmatrix} -1 & -\frac{s}{\varpi+\alpha\beta+1} \\ 0 & \delta\left(n + \frac{\beta}{\alpha\beta+1} - \frac{q}{\delta}\right) \end{pmatrix},$$

which has two positive eigenvalues so E_1 is said to be stable if $\delta\left(n + \frac{\beta}{\alpha\beta+1}\right) < q$ and saddle if $\delta\left(n + \frac{\beta}{\alpha\beta+1}\right) > q$.

3) Predator-persistence equilibrium $E_2 = (0, n\alpha\beta + \beta)$: The Jacobian is

$$J_{E_2} = \begin{pmatrix} 1 - \dfrac{s(n\alpha\beta+\beta)}{\varpi+\alpha\beta} & 0 \\ \delta(n\alpha\beta+\beta)\left(\frac{n}{\alpha\beta} - \frac{q}{\delta}\right) & -\dfrac{\delta(n\alpha+1)}{\alpha} \end{pmatrix}.$$

The eigenvalues are:

$$\lambda_1 = -\frac{\delta(n\alpha+1)}{\alpha} < 0, \quad \lambda_2 = 1 - \frac{s(\alpha\beta+\beta)}{\varpi+\alpha\beta}.$$

Thus, E_2 is:

- stable if $\lambda_2 < 0 \Rightarrow \varpi < s(\alpha\beta + \beta) - \alpha\beta$ and $C > 0$,
- a saddle if $\lambda_2 > 0$ or $C < 0$, indicating at least one interior equilibrium exists.

4) To examine the stability of the interior equilibrium (u^*, v^*), we compute the Jacobian matrix of system (2.1) evaluated at this non-trivial point. The matrix is given by:

$$J_{E^*} = \begin{pmatrix} -u^* + \dfrac{sv^*u^*}{(\varpi+\alpha\beta+u^*)^2} & -\dfrac{su^*}{\varpi+\alpha\beta+u^*} \\ \delta v^*\left(\dfrac{v^*-\beta}{(\alpha\beta+u^*)^2} - \dfrac{q}{\delta}\right) & -\dfrac{\delta v^*}{(\alpha\beta+u^*)} \end{pmatrix}.$$

To find the conditions under which $\mathrm{Tr}(J) < 0$ and $\det(J) > 0$, we will substitute the expressions for $\mathrm{Tr}(J)$ and $\det(J)$ into the inequalities and solve for u^* and v^*.
Given the expressions we derived earlier for $\mathrm{Tr}(J)$:

$$Tr(J) = u\left(-1 + \frac{sv}{(m + \alpha\beta + u)^2}\right) - \delta\frac{v^*}{\alpha\beta + u^*}.$$

$Tr\ J < 0$ if

$$s < \left(u^* + \frac{\delta v^*}{(\alpha\beta + u^*)}\right)\left(\frac{(\varpi + \alpha\beta + u^*)^2}{u^* v^*}\right). \tag{2.9}$$

$det\ J > 0$, if

$$\delta u^* v^* + \left(\frac{s\delta v^* u^*}{\varpi + \alpha\beta + u^*}\right)\frac{v^* - \beta}{(\alpha\beta + u^*)} > \frac{s\delta u^* (v^*)^2}{(\varpi + \alpha\beta + u^*)^2} + \frac{qs\delta v^* u^* (\alpha\beta + u^*)}{\delta (\varpi + \alpha\beta + u^*)},$$

$$\frac{\delta(\varpi + \alpha\beta + u^*)^2 (u^* + \alpha\beta)}{q(u^*)^3 + (3\alpha\beta + \varpi) q(u^*)^2 + (3q\alpha^2\beta + \delta + 2q\varpi\alpha)\beta u^* + (q\alpha^3\beta^2 + q\varpi\alpha^2\beta + \delta\alpha\beta + \varpi\delta)\beta - \varpi\delta v^*} > s. \tag{2.10}$$

□

Adding anti-predator behavior to the model helps turn an unstable system into a stable one by balancing predation dynamics. This shows that the effect of the anti-predator response rate within the model system can shift the dynamics from chaotic cycles to a more stable equilibrium, see Figure 1.

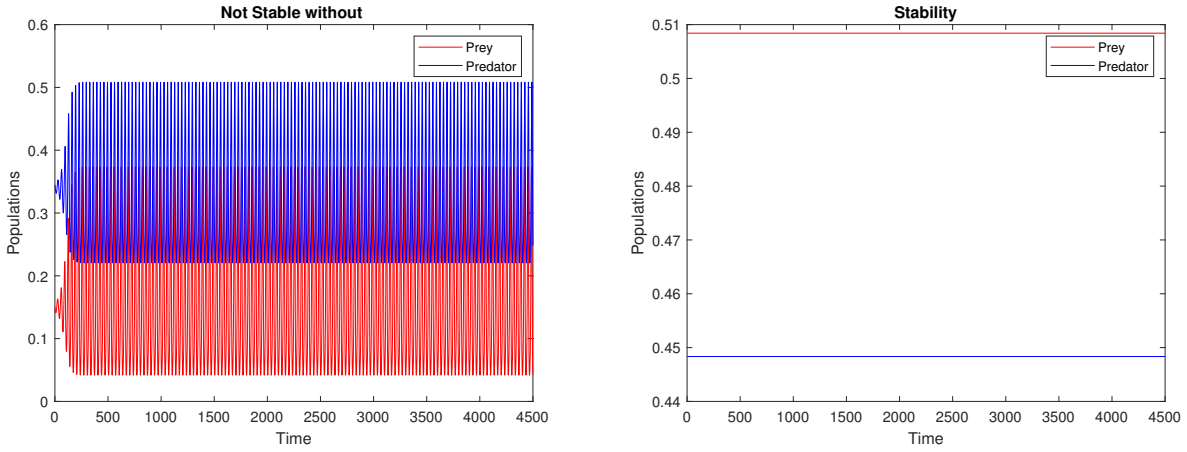

Figure 1. A comparison of system dynamics 2.1 with and without anti-predator behavior. In the absence of anti-predator effects (left panel), the system displays instability. However, when a moderate level of anti-predator response is introduced (right panel), the dynamics become stable. The specific parameter values used in these simulations are listed in Table 2.

2.2. Cyclical dynamics

This section analysis focuses on identifying the conditions that generate cyclic population dynamics in the predator-prey system (Eq (2.1)). As a foundation for this investigation, we first demonstrate that all solutions remain bounded over time—a crucial requirement for biological plausibility. Establishing these bounds not only validates the model's predictions but also provides essential context for understanding how anti-predator behavior influences the system's dynamics.

We now state our boundedness result for system (2.1).

Proposition 2.2. *The region* $\Phi = \{(u(t), v(t)) : 0 \leq u(t) \leq 1, 0 \leq v(t) \leq \left(n + \frac{1}{\alpha}\right)(\alpha\beta + 1)\}$ *is positively invariant and attracts all trajectories starting in the interior of the positive quadrant.*

Proof. Suppose $u(t)$ and $v(t)$ represent positive solutions to system (2.1). Under these conditions, it follows straightforwardly that, from the prey equation u,

$$\frac{du}{dt} \leq (1 - u(t))\, u\,(t)\,.$$

From [34], we have that

$$\lim_{t\to+\infty} \sup u(t) \leq 1. \tag{2.11}$$

Therefore, given any $\epsilon > 0$, we can find a time $T_1 > 0$ such that for all $t > T_1$, the following holds:

$$u(t) \leq 1 + \epsilon, \qquad \text{for } t \geq T_{1.} \tag{2.12}$$

Now from the predator equation, we have

$$\frac{dv\,(t)}{dt} \leq \left[\delta\left(n + \frac{\beta}{\alpha\beta}\right) - \left(\frac{\delta}{\alpha\beta + u(t)}\right) v\,(t)\right] v\,(t)\,.$$

Substituting (2.12) into the last equation gives:

$$\frac{dv\,(t)}{dt} \leq \left[\delta\left(n + \frac{1}{\alpha}\right) - \left(\frac{\delta}{\alpha\beta + 1 + \epsilon}\right) v\,(t)\right] v\,(t)\,.$$

Based on proposition [34], we get

$$\lim_{t\to+\infty} \sup v(t) \leq \left(n + \frac{1}{\alpha}\right)(\alpha\beta + 1 + \epsilon)\,.$$

As ϵ approaches zero, the system simplifies to the following form:

$$\lim_{t\to+\infty} \sup v(t) \leq \left(n + \frac{1}{\alpha}\right)(\alpha\beta + 1)\,.$$

For every $\epsilon > 0$, there is a corresponding time T_2 after which the condition is satisfied to within ϵ.

$$v(t) \leq \left(n + \frac{1}{\alpha}\right)(\alpha\beta + 1) + \epsilon, \quad \text{for } t \geq T_2. \tag{2.13}$$

As ϵ approaches zero, the system simplifies to the following form:

$$v(t) \leq \left(n + \frac{1}{\alpha}\right)(\alpha\beta + 1), \quad \text{for } t \geq T_2. \tag{2.14}$$

□

The system ensures biologically realistic dynamics where neither the prey nor predator populations become negative or grow without bound. Under certain parametric conditions, it can be demonstrated that model (2.1) admits a closed loop. This result is formalized in the following:

Proposition 2.3. *Consider the predator-prey system* (2.1)*, which admits a positive interior equilibrium* $E^* = (u^*, v^*)$*. The behavior of the system near this equilibrium depends on the growth rate parameter s. Specifically, when s meets the following condition:*

$$s > \left(u^* + \frac{\delta v^*}{\alpha\beta + u^*}\right)\left(\frac{(\varpi + \alpha\beta + u^*)^2}{u^* v^*}\right), \tag{2.15}$$

the system guarantees the existence of at least one non-trivial periodic orbit located strictly inside the positive quadrant $\mathbb{R}^2_+$.

Proof. Under condition (2.15), linear stability analysis shows $\mathrm{Tr}(J(E^*)) > 0$ is positive at E^*, while the determinant remains positive indicating E^* is an unstable focus. Since Proposition 2.2 establishes that all solutions are bounded in $\mathbb{R}^2_+$, Poincaré-Bendixson theorem [35], implies that the system must exhibit a limit cycle surrounding this equilibrium. □

The results indicate that a stable periodic solution arises in the system model. When the anti-predator rate is weak and the supplementary food level is moderate, predators and prey can settle into repeated population swings rather than equilibrium. This dynamic is often observed in natural predator-prey interactions and aligns with known ecological patterns.

We will explore these effects further through bifurcation analysis in the next section.

2.3. Global stability

The primary purpose of incorporating the anti-predator mechanism is to enhance predator efficiency, enabling predators to drive pest populations to die out. Without this mechanism, prey extinction inevitably leads to predator extinction, and the origin $(0, 0)$ remains unstable. Yet, with the addition of anti-predator behavior alongside additional food resources, we observe the appearance of the equilibrium point $E_1 = (0, v^*)$. This prompts further investigation into its long-term behavior. Specifically, it is important to examine whether this equilibrium is globally stable or acts as an attractor for nearby trajectories in the system, as illustrated in Figure 2. We formalize this result in the following theorem:

Theorem 2.4 (Pest eradication condition)**.** *Consider the predator–pest model described by system* (2.1)*. Suppose the parameters* s, ω, n*, along with the supplementary food quality* $\frac{1}{\alpha}$ *and quantity* β*, satisfy the inequality* $\delta n > q$*.*

If the following condition holds:

$$\frac{\omega + \alpha\beta + u(t)}{v(t)} < \frac{(\omega + \alpha\beta + 1)\delta}{(\delta n - q)\alpha\beta} < s,$$

then the pest-free equilibrium $(0, v^*)$ *is globally asymptotically stable. In other words, under these parameter restrictions, the pest population will eventually be eliminated regardless of the initial state.*

Proof. To ensure the pest population declines to zero, we examine the pest equation. A guarantee for pest population elimination is that its per capita growth rate remains negative over time.

$$u(t) < \frac{su(t)v(t)}{\omega + \alpha\beta + u(t)}, \tag{2.16}$$

or equivalently

$$\frac{\omega + \alpha\beta + u(t)}{v(t)} < s. \tag{2.17}$$

By examining the predator equation and applying a standard comparison argument, we can derive the following result. This comparison allows us to estimate the predator's behavior by relating it to a simpler or known differential inequality.

$$\frac{dv}{dt} \geq \delta v(t)\left(n + \frac{\beta}{\alpha\beta + u(t)} - \frac{v(t)}{\alpha\beta + u(t)}\right) - qu(t)v(t), \tag{2.18}$$

$$\frac{dv}{dt} \geq v(t)\left((\delta n - q) - \frac{\delta}{\alpha}v(t)\right). \tag{2.19}$$

Thus one has,

$$\lim_{t\to+\infty} \inf v(t) \geq \frac{(\delta n - q)\alpha}{\delta}, \tag{2.20}$$

and using this in Eq (2.17) yields

$$\frac{\omega + \alpha\beta + u(t)}{v(t)} < \frac{(\omega + \alpha\beta + u)\delta}{(\delta n - q)\alpha} < \frac{(\omega + \alpha\beta + 1)\delta}{(\delta n - q)\alpha}. \tag{2.21}$$

Thus if α, β satisfy

$$\frac{(\omega + \alpha\beta + 1)\delta}{(\delta n - q)\alpha} < s, \tag{2.22}$$

then one has

$$\frac{\omega + \alpha\beta + u(t)}{v(t)} < \frac{(\omega + \alpha\beta + 1)\delta}{(\delta n - q)\alpha} < s, \tag{2.23}$$

which implies

$$\lim_{t\to+\infty} u(t) \to 0, \lim_{t\to+\infty} v(t) \to v^*, \tag{2.24}$$

for any initial condition u_0, v_0. □

We now show that it is always possible to choose parameters that guarantee pest eradication. If $s > \frac{\delta}{n-q}$, then for any fixed food quality α, we can select β and q to satisfy the inequality above. In other words, by adjusting the level of supplementary food and the strength of prey defense, one can enforce pest extinction regardless of the starting conditions.

Proposition 2.5. *If s satisfies $s > \frac{\delta}{\delta n - q}$, then for any given additional food quality $\frac{1}{\alpha}$, $\exists\ \beta$ and an anti-predator rate q such that pest eradication is ensured for any initial condition.*

Proof. Note that

$$\frac{(\omega + \alpha\beta + 1)\,\delta}{(\delta n - q)\,\alpha} = \left(\frac{\delta}{\delta n - q}\right)\left(\frac{\omega + \alpha\beta + 1}{\alpha}\right). \tag{2.25}$$

Given that the inequality $s > \frac{\delta}{\delta n - q}$ holds, we proceed under the assumption that this condition is satisfied throughout the analysis. It must be that $s = \frac{\delta}{\delta n - q} + G$, depending on the value of G, whether it is relatively small or considerably large

At this stage, we proceed by selecting parameters δ, n and the anti-predator rate q large or small as required, such that

$$\left(\frac{\delta}{\delta n - q}\right)\left(\frac{\omega + \alpha\beta + 1}{\alpha}\right) < \frac{\delta}{\delta n - q} + G = s. \tag{2.26}$$

This conclusion follows directly from the conditions established in Theorem 2.4, which completes the argument. □

This result confirms that combining supplemental feeding with anti-predator behavior can eliminate the pest population entirely, provided key parameters are chosen appropriately. The critical factor is maintaining a high enough predation rate s while ensuring that predator growth outpaces the negative effects of prey defense.

This global attractivity will be validated in simulations and provides a theoretical baseline for effective pest control strategies.

Remark 2.6. *By adjusting the anti-predator rate q, it is always possible to drive the pest population to extinction, regardless of the initial state of the system, as long as the condition*

$$s > \frac{\delta}{\delta n - q}$$

is satisfied.

3. Bifurcation analysis

This section focuses on the local bifurcation analysis of the model. We derive the necessary conditions under which bifurcations occur, highlighting how the system's qualitative behavior changes in response to parameter variations. Conditions are derived for Hopf bifurcations and saddle-node bifurcations. These forms help determine the nature of equilibria at critical parameter values.

3.1. Hopf-bifurcation analysis

A Hopf bifurcation arises when a previously stable equilibrium loses its stability, leading to the emergence of a periodic orbit (also known as a limit cycle). In this analysis, we consider the predation rate s as the bifurcation parameter, while all other parameters remain fixed.

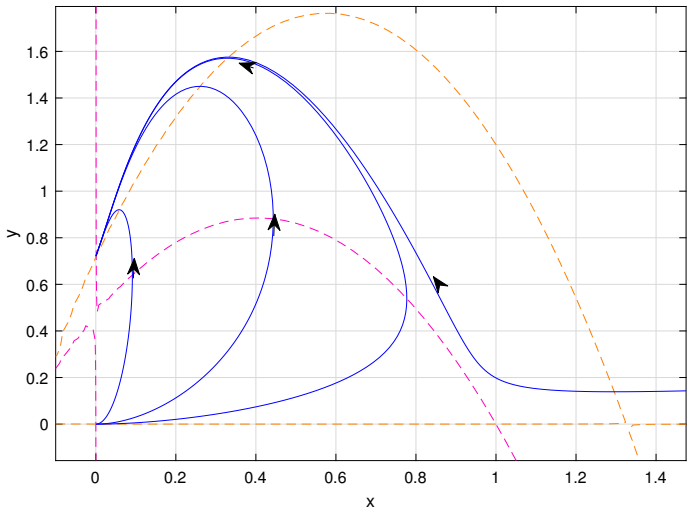

Figure 2. This figure provides a numerical confirmation of Theorem 2.4. It demonstrates that the system defined by (2.1) can exhibit a globally attracting equilibrium where the pest population goes extinct, represented by the point $(0, v^*)$. For the specific parameter values applied in this simulation, refer to Table 2.

Let $E^* = (u^*, v^*)$ denote the interior equilibrium point. Evaluating the Jacobian matrix at this point, we observe that both its trace and determinant depend on the parameter s.

Theorem 3.1. *[36] The necessary and sufficient conditions for the occurrence of a Hopf bifurcation from the equilibrium E^* exists, $s = s_c$, such that*

1) $Tr\, J(s_c) = 0$,

2) $\left[\frac{d\,\mathrm{Re}(\lambda(s))}{ds}\right]_{s=s_c} \neq 0$.

Proof. The characteristic equation of the Jacobian matrix can be simplified to: □

$$\lambda^2 + b(s)\lambda + c(s) = 0.$$

At the bifurcation point, the trace of the Jacobian matrix becomes zero. At this point, the characteristic equation of the linearized system has purely imaginary roots at

$$s_c = \left(u^* + \frac{\delta v^*}{(\alpha\beta + u^*)}\right)\left(\frac{(\varpi + \alpha\beta + u^*)^2}{u^* v^*}\right).$$

$\mathrm{Tr}(J)\,|_{E^*} = 0$, which means $b(s_c) = 0$. Therefore, the characteristic equation becomes:

$$\lambda^2 + c(s_c) = 0,$$

In this case, both eigenvalues become purely imaginary when the determinant of the Jacobian matrix evaluated at E^* is positive, i.e., $\det(J)\big|_{E^*} > 0$.

As a result, applying the implicit function theorem shows that a Hopf bifurcation takes place. This leads to the emergence of a periodic orbit, coinciding with a change in the stability of the equilibrium point E^*.

It can be demonstrated that, under specific parameter conditions, the interior equilibrium E^* undergoes a supercritical Hopf bifurcation, leading to the emergence of a stable limit cycle. For a fixed set of parameters $\alpha, \beta, \delta, \varpi, n, q$, and s, there exists a critical value s_c such that the Jacobian matrix satisfies $J(s_c) = 0$ and the transversality condition

$$\frac{d}{ds}\,\mathrm{Re}(\lambda(s))\Big|_{s=s_c} \neq 0,$$

where $\lambda(s)$ denotes the eigenvalues of the linearized system. This situation is illustrated in Figure 3.

By applying the implicit function theorem, it follows that a Hopf bifurcation takes place at $s = s_c$. As a result, the equilibrium E^* loses stability and a periodic orbit arises in its vicinity, marking the birth of sustained oscillations in the system.

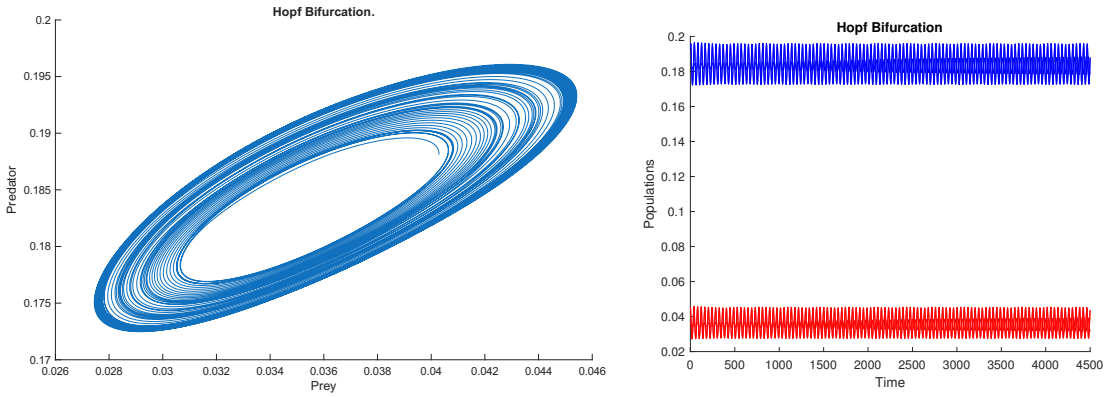

Figure 3. This figure illustrates system (2.1) exhibiting a Hopf bifurcation. Parameter values used in the simulation are listed in Table 2.

3.2. Saddle-node bifurcation

For system (2.1), the number of interior equilibrium points depends on the chosen parameter values. Specifically, it is possible to have two distinct interior equilibria, denoted by

$$E_1^* = (u_1^*, v_1^*) \quad \text{and} \quad E_2^* = (u_2^*, v_2^*)\,.$$

As parameters vary, these two equilibrium points may approach each other and eventually merge into a single, unique interior equilibrium

$$\bar{E} = (\bar{u}, \bar{v})\,.$$

This merging occurs when the conditions

$$B > 0, \quad B^2 = 4AC, \quad \text{and} \quad \frac{-B}{2A} > 0$$

are satisfied, characterizing a saddle—node bifurcation.

At the point $\bar{E}$, the Jacobian matrix has a non-hyperbolic eigenvalue, which means linear stability analysis is inconclusive. This signals the possibility of a bifurcation near this equilibrium. Fixing all other parameters, the two interior equilibria E_1^* and E_2^* collide via a saddle-node bifurcation, leading to qualitative changes in the system's dynamics.

Such bifurcations are important as they often mark the transition between different stability regimes, indicating the onset or disappearance of equilibrium points depending on parameter values.

The value $n^{[sn]}$ satisfies the inequality

$$n^{[sn]} < \frac{\alpha\beta qs + \delta(-\alpha\beta - \varpi + 1)}{\delta s},$$

provided that $\delta - qs > 0$. The critical values of $n^{[sn]}$ are given by

$$n^{[sn]} = \frac{\delta\left(\alpha\beta\delta - \alpha\beta qs - \delta\varpi + \delta\right) \pm 2\sqrt{-\delta^3(\delta - qs)(\alpha\beta\varpi - \beta s + \varpi)}}{\delta^2 s}.$$

At these critical values, the system undergoes a saddle—node bifurcation, where two equilibrium points collide and annihilate each other.

The parametric surface

$$\Gamma = \left\{(\alpha, \beta, \delta, q, \varpi, n, s) \in \mathbb{R}_+^7 \ : \ \frac{-B}{2A} > 0 \text{ and } B^2 = 4AC\right\}$$

defines the saddle—-node bifurcation manifold in the parameter space.

This surface marks the boundary between different dynamic behaviors of the system, where a qualitative change in the number of equilibrium points occurs.

This critical value corresponds to the point where the two equilibrium points collide, resulting in a saddle-node bifurcation.

Theorem 3.2. *System* (2.1) *experiences a saddle—node bifurcation around* $\bar{E}$ *at* $n^{[sn]}$, *where* $n^{[sn]} = \frac{\delta(\alpha\beta\delta - \alpha\beta qs - \delta\omega + \delta) \pm 2\sqrt{-\delta^3(\delta - qs)(\alpha\beta\omega - \beta s + \omega)}}{\delta^2 s}$ *and* $n^{[sn]} < (>) \frac{\alpha\beta qs + \delta(-\alpha\beta - \omega + 1)}{\delta s}$, *if* $\delta - qs > (<)\ 0$ *such that* $\frac{-B}{2A} > 0$, $B^2 = 4AC$, *and* $trJ_{\bar{E}} < 0$.

These provide the values of n under the given conditions.

Proof. As stated in Sotomayor's theorem [37, 38], a saddle-node bifurcation occurs when one of the eigenvalues of the Jacobian matrix $J_{\bar{E}}$, evaluated at the equilibrium point $\bar{E}$, becomes zero if and only if $\det J_{\bar{E}} = 0$, which corresponds to $n = n^{[sn]}$. This signals a change in the stability structure of the system and typically marks the merging or disappearance of two equilibrium points. The other eigenvalue, represented by $\operatorname{tr} J_{\bar{E}}$ and evaluated at $n = n^{[sn]}$, must have a negative real part for the occurrence of a saddle-node bifurcation (Sotomayor, 1973). Therefore, the condition $\operatorname{tr} J_{\bar{E}} < 0$ must hold.

Let $V = \begin{pmatrix} v_1 \\ v_2 \end{pmatrix}$ and $W = \begin{pmatrix} w_1 \\ w_2 \end{pmatrix}$ be the eigenvectors corresponding to the eigenvalue 0 of the Jacobian matrix $J_{\bar{E}}$ and its transpose, respectively. These eigenvectors satisfy the relations:

$$v_1 = -\frac{j_{12}v_2}{j_{11}} = -\frac{j_{22}v_2}{j_{21}}, \quad w_1 = -\frac{j_{21}w_2}{j_{11}} = -\frac{j_{22}w_2}{j_{12}},$$

where $v_2, w_2 \in \mathbb{R} \setminus \{0\}$.

Let the system be described by:

$$F = \begin{bmatrix} F_1 \\ F_2 \end{bmatrix} = \begin{bmatrix} u(1-u) - \frac{suv}{\varpi+\alpha\beta+u} \\ \delta v\left(n + \frac{\beta - v}{\alpha\beta+u} - \frac{q}{\delta}u\right) \end{bmatrix},$$

and let $U = \begin{pmatrix} u \\ v \end{pmatrix}$.

The partial derivative of F with respect to n is:

$$\frac{\partial F}{\partial n} = \begin{bmatrix} 0 \\ \delta v \end{bmatrix}.$$

The transversality condition is satisfied if:

$$W^T \cdot \frac{\partial F}{\partial n} = W^T \begin{bmatrix} 0 \\ \delta v \end{bmatrix} = w_1 \cdot 0 + w_2 \cdot \delta v = \delta w_2 v \neq 0.$$

Additionally, the second derivative of F satisfies:

$$W^T \left[D^2 F(U, n^{[sn]}) \cdot (V, V)\right] \neq 0.$$

According to Sotomayor's theorem, a saddle-node bifurcation occurs in the system when the parameter n reaches the critical value $n = n^{[sn]}$. At this point, two positive interior equilibria merge and disappear at the point $\bar{E}$, marking a qualitative change in the system's dynamics. □

This type of bifurcation signals a critical threshold. If parameters fall beyond this point, the system can lose all interior steady states, leading to extinction or uncontrolled growth. For biological control, this means that predator-prey balance becomes impossible if conditions like the predator growth rate or food quality fall below a safe limit.

Remark 3.3. *In this study, the bifurcation analysis has been restricted to Hopf and saddle-node bifurcations, as they determine the onset of oscillatory dynamics and the coexistence of multiple equilibria in the system.*

We note that transcritical bifurcations may arise in connection with the equilibrium E_2, where an exchange of stability between equilibria can occur. A detailed analytical investigation of such bifurcations is not included in the present work and is left for future research.

4. Turing instability

Turing instability, also referred to as diffusion-driven instability, occurs when a spatially homogeneous equilibrium that is stable in the corresponding ordinary differential equation (ODE) system becomes unstable once diffusion terms are introduced in the partial differential equation (PDE) formulation. In this scenario, diffusion—rather than stabilizing the system—triggers pattern formation by destabilizing the previously stable interior equilibrium. A detailed discussion of this mechanism can be found in [39].

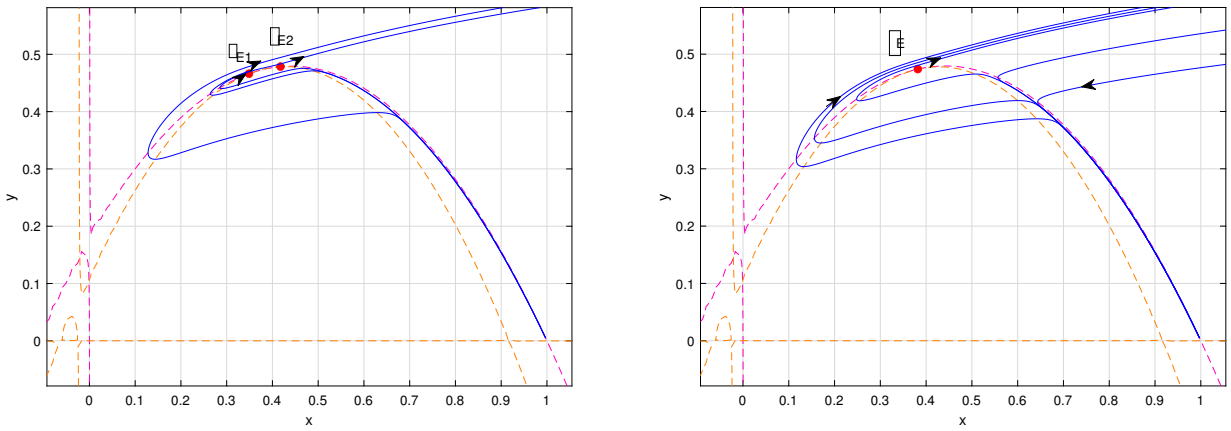

Figure 4. These plots illustrate a saddle-node bifurcation. As the parameter n increases from panel (a) to panel (b), the system undergoes a qualitative change. In panel (a), two distinct interior equilibrium points are visible. As n increases, these equilibria approach each other, eventually merging into a single point. This coalescence results in the disappearance of the two distinct equilibria and the emergence of a single, degenerate equilibrium, as shown in panel (b). The values of all parameters used in this simulation are listed in Table 2.

To extend the previously introduced ODE models into a spatially explicit framework, we incorporate the movement of both predator and prey across space. In real ecosystems, individuals often move in search of food, more favorable environmental conditions, or social interactions such as locating mates [39]. These behaviors result in spatial redistribution, which must be captured to more accurately reflect the system's dynamics. Random movement is a common approach to represent such dispersal patterns in mathematical models.

To account for spatial movement, the model incorporates diffusion under the assumption that individuals disperse uniformly in all directions. This assumption leads to the addition of standard diffusion terms, resulting in the following extended system:

$$\left.\begin{aligned} u_t &= D_u u_{xx} + u\,(1-u) - \frac{suv}{\varpi + \alpha\beta + u}, \\ v_t &= D_v v_{xx} + \delta v\left(n + \frac{\beta}{\alpha\beta + u} - \frac{v}{\alpha\beta + u}\right) - quv \end{aligned}\right\}. \tag{4.1}$$

The domain for the model is $\Omega \subset \mathbb{R}^1$, which is assumed to be bounded. Neumann boundary conditions, $u_x = v_x = 0$ for $x \in \partial\Omega$ with $\Omega = [0, \pi]$, are imposed alongside appropriate initial conditions. These boundary conditions are selected to emphasize the self-organization of patterns in the system, as zero-flux conditions ensure no external input or influence affects the dynamics.

In this model, $u(x, t)$ represents the prey population density at time t. The growth of the prey is assumed to follow logistic dynamics, meaning it increases when the population is small and slows down as it approaches the environmental carrying capacity. $v(x, t)$ denotes the population density of the

predator at position x and time t preying on the prey population. This framework enables the analysis of diffusion-driven dynamics and the emergence of spatial patterns arising from the interactions between the two species.

Our goal is to examine the specific conditions that lead to the formation of Turing patterns in the system described by equation (4.1). To do this, we analyze how diffusion-driven instabilities influence the spatial dynamics of the model. Specifically, we focus on identifying the conditions under which the introduction of an anti-predator alone can lead to the formation of Turing patterns.

To achieve this, we begin by linearizing the model system around its homogeneous steady state (u^*, v^*), where (u^*, v^*) represents the equilibrium with an anti-predator. This is done by introducing spatially and temporally dependent fluctuations to the steady state.

To clearly identify when Turing instability arises, we adopt the standard analytical approach introduced by [39]. This method provides a structured path for deriving the necessary mathematical conditions. The outcome of this process is summarized in the theorem below, which presents the key results used in our analysis.

Theorem 4.1 (Turing instability criterion)**.** *Let (u^*, v^*) be a spatially uniform equilibrium of the system. Consider the Jacobian matrix of the reaction terms evaluated at this point:*

$$\mathbf{J} = \begin{bmatrix} J_{11} & J_{12} \\ J_{21} & J_{22} \end{bmatrix}.$$

Suppose the diffusion coefficients are D_u and D_v. The following conditions must hold:

$$\begin{aligned} &J_{11} + J_{22} < 0, \\ &J_{11}J_{22} - J_{21}J_{12} > 0, \\ &D_v J_{11} + D_u J_{22} > 0, \\ &(D_v J_{11} + D_u J_{22})^2 - 4D_u D_v (J_{11}J_{22} - J_{21}J_{12}) > 0. \end{aligned}$$

When these inequalities are satisfied, the equilibrium (u^*, v^*) is stable if diffusion is ignored but becomes unstable once diffusion is included. This phenomenon, where diffusion destabilizes a previously stable state, is known as Turing instability.

Building on the earlier findings, we derive a simple but important condition that further restricts the parameters under which Turing instability can arise.

Proposition 4.2 (Necessary condition for Turing instability)**.** *Consider the spatially homogeneous equilibrium point (u^*, v^*) of the system. Suppose this equilibrium is stable when diffusion effects are ignored but becomes unstable once diffusion is introduced. Under these circumstances, the Jacobian matrix of the reaction terms,*

$$\mathbf{J} = \begin{bmatrix} J_{11} & J_{12} \\ J_{21} & J_{22} \end{bmatrix},$$

must satisfy at least one of the following conditions:

1) The diagonal entry J_{11} is negative while the off-diagonal entry J_{21} is positive.

2) The diagonal entry J_{11} is positive and J_{22} is negative.

These conditions are necessary for the system to exhibit Turing-type instability, where diffusion destabilizes an otherwise stable uniform state.

Since Turing patterns emerge from destabilization of the homogeneous state, we first investigate the linear stability. By evaluating the Jacobian matrix at the homogeneous equilibrium point, we can analyze the system's local stability and determine how small perturbations around this equilibrium evolve.

For the solution (u^*, v^*) of (4.1) the Jacobian matrix is given by

$$J_{E^*} = \begin{pmatrix} -u^* + \dfrac{su^*v^*}{(\varpi + \alpha\beta + u^*)^2} & -\dfrac{su^*}{\varpi + \alpha\beta + u^*} \\ \delta v^* \left(\dfrac{v^* - \beta}{(\alpha\beta + u^*)^2} - \dfrac{q}{\delta} \right) & -\dfrac{\delta v^*}{(\alpha\beta + u^*)} \end{pmatrix}.$$

System (4.1) plays a crucial role in shaping the Turing dynamics, provided it meets the necessary criteria to induce spatial patterning and instabilities, and it is essential that $J_{11} > 0$. Clearly, if $J_{11} < 0$, Turing instability cannot occur. Although $J_{11} > 0$ is a required condition for Turing instability, it alone does not ensure that instability will occur. This criterion signals only the possibility of Turing patterns emerging, but additional conditions must be satisfied for instability to actually develop. We summarize our findings in the following theorem.

Theorem 4.3. *Consider the point (u^*, v^*), which represents a spatially homogeneous equilibrium solution of system* (4.1)*. Suppose the parameters $\{\alpha, \varpi, \beta, \delta, s, n, q\}$ are all strictly positive and satisfy the following set of inequalities.*

At the equilibrium (u^*, v^*), let the Jacobian matrix be

$$\mathbf{J} = \begin{bmatrix} J_{11} & J_{12} \\ J_{21} & J_{22} \end{bmatrix},$$

and denote the diffusion coefficients by D_u and D_v. These quantities satisfy the conditions:

$$\frac{(\varpi + \alpha\beta + u^*)^2}{v^*} < s < \min\{K_1, K_2\},$$

$$D_v \left(-u^* + \frac{su^*v^*}{(\varpi + \alpha\beta + u^*)^2} \right) > D_u \left(\frac{\delta v^*}{\alpha\beta + u^*} \right),$$

and

$$\left[D_v \left(-u^* + \frac{su^*v^*}{(\varpi + \alpha\beta + u^*)^2} \right) - D_u \left(\frac{\delta v^*}{\alpha\beta + u^*} \right) \right]^2 >$$

$$4D_uD_v \left[\left(u^* - \frac{sv^*u^*}{(\varpi + \alpha\beta + u^*)^2} \right) \left(\frac{\delta v^*}{\alpha\beta + u^*} \right) + \left(\frac{v^* - \beta}{(\alpha\beta + u^*)^2} - \frac{q}{\delta} \right) \left(\frac{\delta su^*v^*}{\varpi + \alpha\beta + u^*} \right) \right].$$

Here, the constants K_1 and K_2 are given by the expressions:

$$K_1 = \left(u^* + \frac{\delta v^*}{\alpha\beta + u^*}\right)\left(\frac{(\varpi + \alpha\beta + u^*)^2}{u^* v^*}\right),$$

$$K_2 = \frac{\delta(\varpi + \alpha\beta + u^*)^2(u^* + \alpha\beta)}{q(u^*)^3 + q(3\alpha\beta + \varpi)(u^*)^2 + \beta(3q\alpha^2\beta + \delta + 2q\varpi\alpha)u^* + \beta(q\alpha^3\beta^2 + q\varpi\alpha^2\beta + \delta\alpha\beta + \varpi\delta) - \varpi\delta v^*}.$$

Under these assumptions, the equilibrium (u^*, v^*) is linearly stable if diffusion is absent, but becomes linearly unstable once diffusion effects are included.

Proof. Let (u^*, v^*) denote the spatially homogeneous equilibrium of system (4.1). We first analyze the stability of this equilibrium for the corresponding kinetic system obtained by neglecting the diffusion terms.

The Jacobian matrix evaluated at (u^*, v^*) is

$$J = \begin{bmatrix} J_{11} & J_{12} \\ J_{21} & J_{22} \end{bmatrix}.$$

According to Theorem 4.1, the equilibrium of the reaction system is locally asymptotically stable provided that

$$\mathrm{Tr}(J) = J_{11} + J_{22} < 0, \qquad \det(J) = J_{11}J_{22} - J_{12}J_{21} > 0.$$

Using expressions (2.7)–(2.8) from Theorem 2.1, the trace condition $\mathrm{Tr}(J) < 0$ is satisfied whenever

$$s < \left(u^* + \frac{\delta v^*}{\alpha\beta + u^*}\right)\left(\frac{(\varpi + \alpha\beta + u^*)^2}{u^* v^*}\right) = K_1.$$

Similarly, the determinant condition $\det(J) > 0$ holds provided that

$$s < \frac{\delta(\varpi + \alpha\beta + u^*)^2(u^* + \alpha\beta)}{q(u^*)^3 + q(3\alpha\beta + \varpi)(u^*)^2 + \beta(3q\alpha^2\beta + \delta + 2q\varpi\alpha)u^* + \beta(q\alpha^3\beta^2 + q\varpi\alpha^2\beta + \delta\alpha\beta + \varpi\delta) - \varpi\delta v^*} = K_2.$$

In addition, Proposition 4.2 shows that a necessary requirement for diffusion-driven instability is $J_{11} > 0$. From the explicit expression of J_{11}, this condition is satisfied whenever

$$\frac{(\varpi + \alpha\beta + u^*)^2}{v^*} < s.$$

Consequently, if

$$\frac{(\varpi + \alpha\beta + u^*)^2}{v^*} < s < \min\{K_1, K_2\},$$

then the equilibrium (u^*, v^*) is locally asymptotically stable for the reaction system in the absence of diffusion.

We now consider the full reaction-diffusion system. Following the classical Turing instability criterion, diffusion destabilizes the equilibrium if

$$D_v J_{11} + D_u J_{22} > 0$$

and

$$(D_v J_{11} + D_u J_{22})^2 > 4 D_u D_v (J_{11} J_{22} - J_{12} J_{21}).$$

Substituting the entries of the Jacobian matrix yields

$$D_v \left(-u^* + \frac{s u^* v^*}{(\varpi + \alpha\beta + u^*)^2} \right) > D_u \left(\frac{\delta v^*}{\alpha\beta + u^*} \right)$$

and

$$\left[D_v \left(-u^* + \frac{s u^* v^*}{(\varpi + \alpha\beta + u^*)^2} \right) - D_u \left(\frac{\delta v^*}{\alpha\beta + u^*} \right) \right]^2 > 4 D_u D_v (J_{11} J_{22} - J_{12} J_{21}).$$

Moreover,

$$J_{11} J_{22} - J_{12} J_{21} = \left(u^* - \frac{s u^* v^*}{(\varpi + \alpha\beta + u^*)^2} \right) \left(\frac{\delta v^*}{\alpha\beta + u^*} \right) + \left(\frac{v^* - \beta}{(\alpha\beta + u^*)^2} - \frac{q}{\delta} \right) \left(\frac{\delta s u^* v^*}{\varpi + \alpha\beta + u^*} \right).$$

Therefore, the equilibrium (u^*, v^*) remains stable for the reaction system but loses stability once diffusion is introduced. Hence diffusion induces instability of the homogeneous state, and the system admits diffusion-driven (Turing) instability. □

If these conditions are met, the steady state (u^*, v^*) transitions from being stable without diffusion to unstable when diffusion is introduced, leading to diffusion-driven (Turing) instability. This instability is key to the emergence of spatial patterns in the system, see Figure 5.

The model shows that anti-predator actions and food supplementation together can drive or suppress these patterns, depending on parameter values. This insight can inform field-based pest management by highlighting the importance of spatial structure in ecological interventions.

5. Discussion and conclusions

This study investigated a modified Holling-Tanner predator-prey model that incorporates supplementary food for predators and anti-predator behavior in prey. The analysis shows how these two ecological mechanisms influence system stability, oscillations, and spatial pattern formation. To strengthen the biological relevance of these findings, we now discuss their implications in real predator-pest systems.

Without anti-predator behavior, the system demonstrates unstable dynamics where predator and prey populations oscillate unpredictably, as illustrated in (Figure 1(a)), this describes repeated pest outbreaks driven by overexploitation followed by predator decline. However, the inclusion of anti-predator behavior stabilizes the system, leading to a steady state equilibrium, as shown in Figure 1(b). This indicates that the equilibrium becomes locally asymptotically stable. In ecological terms, prey reduce their exposure to predation, which lowers the effective interaction strength and suppresses outbreak cycles, leading to a regulated and predictable system.

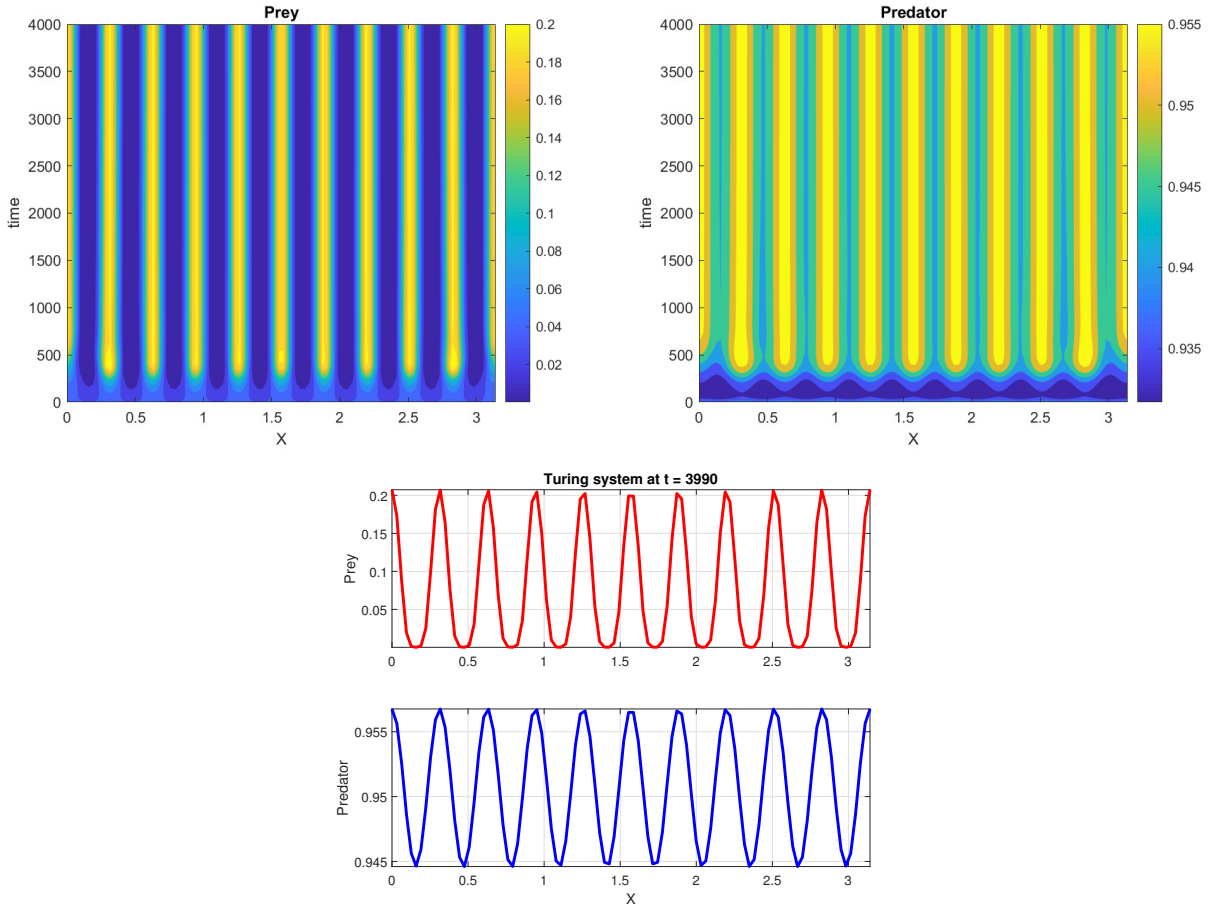

Figure 5. Turing patterns emerging in the predator and pest populations are illustrated for model (4.1). The spatial domain is set as $\Omega = [0, \pi]$. To initiate pattern formation, the spatially uniform steady state is slightly disturbed using a perturbation of the form $\epsilon_1 \cos^2(10x)$, where $\epsilon_1 \ll 1$. The diffusion coefficients are chosen as $D_u = 10^{-5}$ and $D_v = 0.019$. For a full list of parameters used in these simulations, refer to Table 2.

The results, via Theorem 2.4 and Proposition 2.3, show that we have established that anti-predator behavior, combined with supplementary food, ensures pest eradication under appropriate parameter conditions. This result is numerically validated in Figure 2, where the system converges to a globally stable pest extinction state. The sufficient condition $\omega + \alpha\beta + 1 < s$, such that the $(0, v^*)$ state is globally attracting, ensures that that predators can persist on supplementary food while maintaining sufficient pressure on the pest population. This scenario corresponds to successful biological control, where pests are eradicated without causing predator collapse.

Furthermore, we find anti-predator behavior also contributes to the emergence of limit cycles under certain conditions, as formalized in Proposition 2.3 and demonstrated in Figure 3. Here, the system transitions between stable and cyclical behaviors depending on the strength of anti-predator effects and predation parameters. The Hopf bifurcation analysis via Theorem 3.1 confirms that anti-predator behavior plays a critical role in determining whether stable equilibria or oscillatory dynamics emerge, which corresponds to sustained predator–prey cycles, where pest densities rise and

fall in a regular pattern. Such dynamics are commonly observed when prey exhibit partial avoidance behavior that weakens but does not eliminate predator impact. Even a saddle-node bifurcation is possible via Theorem 3.2, as the model suggests that combining moderate supplementary food with realistic anti-predator effects can stabilize dynamics and drive pests to extinction. This reflects integrated pest management strategies, where supplementation helps sustain predators even when prey temporarily decline, but requires careful calibration to avoid reducing predation.

This outcome also reflects threshold phenomena. If predator density is initially too low, pests escape control and establish at high levels. If predator density exceeds a critical threshold, the system shifts to effective control. This highlights the importance of initial releases in biological control programs.

In the spatially explicit model (PDE system), anti-predator behavior influences the emergence of Turing patterns, as demonstrated in Figure 5. The conditions derived in Theorem 4.3 indicate that anti-predator effects, coupled with diffusion, can drive spatial heterogeneity, resulting in pattern formation. This suggests that anti-predator behavior enhances system resilience by promoting predator-prey coexistence in heterogeneous environments. The diffusion extension predicts the emergence of Turing patterns, where prey and predator form spatial clusters. Similar patchy distributions are often observed in greenhouse crops when predators forage unevenly. This spatial heterogeneity is frequently observed in agricultural systems and has direct implications for pest management, as uniform interventions may fail to address localized outbreaks.

These findings suggest that effective pest management requires careful parameter balancing. Moderate supplementary food supports predator persistence, while excessive supplementation may weaken predation pressure. Anti-predator behavior stabilizes dynamics but may also reduce control efficiency if too strong. Spatial effects further indicate that localized strategies may outperform uniform approaches. Future studies should focus on empirical validation and explore additional ecological complexities, such as stochastic effects and environmental variability.

Table 2. Parameters used in the simulations in all figures.

Figure	α	n	β	ϖ	s	δ	q
1(a)	0.5	1.2	0.1	0.08	0.7	0.15	0.0
1(b)	0.5	1.2	0.1	0.08	0.7	0.15	0.17
2	0.5	4	0.24	0.07	0.4	0.35	1.1
3	0.6	2	0.05425789	0.084	0.8	0.07	0.2
4(a)	0.6	1.77668325	0.0542	0.084	0.66	0.1	0.20
4(b)	0.6	1.77668325	0.0542	0.084	0.65	0.1	0.20
5	0.6	2	0.4	0.4	0.7	0.17	0.4

Use of AI tools declaration

The author declares he has not used artificial intelligence (AI) tools in the creation of this article.

Conflict of interest

The author declares there is no conflict of interest.

References

1. D. Pimentel, Environmental and economic costs of the application of pesticides primarily in the United States, *Environ. Dev. Sustain.*, **7** (2005), 229–252. https://doi.org/10.1007/s10668-005-7314-2
2. K. Czaja, K. Góralczyk, P. Struciński, A. Hernik, W. Korcz, M. Minorczyk, et al., Biopesticides-towards increased consumer safety in the European Union, *Pest Manag. Sci.*, **71** (2015), 3–6. https://doi.org/10.1002/ps.3829
3. C. J. Bampfylde, M. A. Lewis, Biological control through intraguild predation: Case studies in pest control, invasive species and range expansion, *Bull. Math. Biol.*, **69** (2007), 1031–1066. https://doi.org/10.1007/s11538-006-9158-9
4. Y. Kang, D. Bai, L. Tapia, H. Bateman, Dynamical effects of biocontrol on the ecosystem: Benefits or harm?, *Appl. Math. Modelling*, **51** (2017), 361–385. https://doi.org/10.1016/j.apm.2017.07.006
5. R. D. Parshad, R. K. Upadhyay, S. Mishra, S. K. Tiwari, S. Sharma, On the explosive instability in a three-species food chain model with modified Holling type IV functional response, *Math. Methods Appl. Sci.*, **40** (2017), 5707–5726. https://doi.org/10.1002/mma.4419
6. R. D. Parshad, S. Bhowmick, E. Quansah, A. Basheer, R. K. Upadhyay, Predator interference effects on biological control: The "paradox" of the generalist predator revisited, *Commun. Nonlinear Sci. Numer. Simul.*, **39** (2016), 169–184. https://doi.org/10.1016/j.cnsns.2016.02.021
7. R. G. V. Driesche, T. S. Bellows, *Biological Control*, Springer Science and Business Media, 2012.
8. E. W. Evans, J. G. Swallow, Numerical responses of natural enemies to artificial honeydew in Utah alfalfa, *Environ. Entomol.*, **22** (1993), 1392–1401. https://doi.org/10.1093/ee/22.6.1392
9. L. A. Canas, R. J. O'Neil, Applications of sugar solutions to maize, and the impact of natural enemies on fall armyworm, *Int. J. Pest Manag.*, **44** (1998), 59–64. https://doi.org/10.1080/096708798228329
10. E. W. Evans, D. R. Richards, Managing the dispersal of ladybird beetles (Col.: Coccinellidae): Use of artificial honeydew to manipulate spatial distributions, *BioControl*, **42** (1997), 93–102. https://doi.org/10.1007/BF02769884
11. M. R. Wade, M. P. Zalucki, S. D. Wratten, K. A. Robinson, Conservation biological control of arthropods using artificial food sprays: Current status and future challenges, *Biol. Control*, **45** (2008), 185–199. https://doi.org/10.1016/j.biocontrol.2007.10.024
12. W. E. Snyder, D. H. Wise, Predator interference and the establishment of generalist predator populations for biocontrol, *Biol. Control*, **15** (1999), 283–292. https://doi.org/10.1006/bcon.1999.0723
13. S. P. Shannon, T. H. Chrzanowski, J. P. Grover, Prey food quality affects flagellate ingestion rates, *Microb. Ecol.*, **53** (2007), 66–73. https://doi.org/10.1007/s00248-006-9140-y

14. G. Saunders, B. Cooke, K. McColl, R. Shine, T. Peacock, Modern approaches for the biological control of vertebrate pests: An Australian perspective, *Biol. Control*, **52** (2010), 288–295. https://doi.org/10.1016/j.biocontrol.2009.06.014

15. A. Tena, A. Pekas, D. Cano, F. L. Wäckers, A. Urbaneja, Sugar provisioning maximizes the biocontrol service of parasitoids, *J. Appl. Ecol.*, **52** (2015), 795–804. https://doi.org/10.1111/1365-2664.12426

16. A. Basheer, E. Quansah, S. Bhowmick, R. D. Parshad, Prey cannibalism alters the dynamics of Holling-Tanner-type predator-prey models, *Nonlinear Dyn.*, **85** (2016), 2549–2567. https://doi.org/10.1007/s11071-016-2844-8

17. A. A. Basheer, R. D. Parshad, E. Quansah, S. Yu, R. K. Upadhyay, Exploring the dynamics of a Holling-Tanner model with cannibalism in both predator and prey population, *Int. J. Biomath.*, **11** (2018), 1850010. https://doi.org/10.1142/S1793524518500109

18. X. Wang, L. Zanette, X. Zou, Modelling the fear effect in predator-prey interactions, *J. Math. Biol.*, **73** (2016), 1179–1204. https://doi.org/10.1007/s00285-016-0989-1

19. G. He, F. Chen, Z. Li, L. Chen, Impact of fear on a stage-structured Lotka-Volterra competition model, *Qual. Theory Dyn. Syst.*, **24** (2025), 170. https://doi.org/10.1007/s12346-025-01331-w

20. K. Put, T. Bollens, F. L. Wäckers, A. Pekas, Type and spatial distribution of food supplements impact population development and dispersal of the omnivore predator Macrolophus pygmaeus (Rambur) (Hemiptera: Miridae), *Biol. Control*, **63** (2012), 172–180. https://doi.org/10.1016/j.biocontrol.2012.06.011

21. P. Turchin, *Complex Population Dynamics: A Theoretical/Empirical Synthesis*, Princeton University Press, 2003.

22. P. D. N. Srinivasu, B. S. R. V. Prasad, M. Venkatesulu, Biological control through provision of additional food to predators: A theoretical study, *Theor. Popul. Biol.*, **72** (2007), 111–120. https://doi.org/10.1016/j.tpb.2007.03.011

23. P. D. N. Srinivasu, B. S. R. V. Prasad, Time optimal control of an additional food provided predator-prey system with applications to pest management and biological conservation, *J. Math. Biol.*, **60** (2010), 591–613. https://doi.org/10.1007/s00285-009-0279-2

24. P. D. N. Srinivasu, B. S. R. V. Prasad, Role of quantity of additional food to predators as a control in predator-prey systems with relevance to pest management and biological conservation, *Bull. Math. Biol.*, **73** (2011), 2249–2276. https://doi.org/10.1007/s11538-010-9601-9

25. H. M. Ulfa, A. Suryanto, I. Darti, Dynamics of Leslie-Gower predator-prey model with additional food for predators, *Int. J. Pure Appl. Math.*, **115** (2017), 751–765. https://doi.org/10.12732/ijpam.v115i2.1

26. R. D. Parshad, S. Wickramsooriya, S. Bailey, A remark on biological control through provision of additional food to predators: A theoretical study, *Theor. Popul. Biol.*, **132** (2020), 60–68. https://doi.org/10.1016/j.tpb.2019.11.010

27. A. Basheer, E. Quansah, R. D. Parshad, The effect of additional food in Holling Tanner type models, *Int. J. Dyn. Control*, **7** (2019), 1195–1212. https://doi.org/10.1007/s40435-019-00580-3

28. Y. Choh, J. Takabayashi, M. W. Sabelis, A. Janssen, Witnessing predation can affect strength of counterattack in phytoseiids with ontogenetic predator-prey role reversal, *Anim. Behav.*, **93** (2014), 9–13. https://doi.org/10.1016/j.anbehav.2014.04.008

29. S. L. Lima, Nonlethal effects in the ecology of predator-prey interactions, *Bioscience*, **48** (1998), 25–34. https://doi.org/10.2307/1313225

30. J. K. Ford, R. R. Reeves, Fight or flight: Antipredator strategies of baleen whales, *Mamm. Rev.*, **38** (2008), 50–86. https://doi.org/10.1111/j.1365-2907.2008.00118.x

31. B. Tang, Y. Xiao, Bifurcation analysis of a predator-prey model with anti-predator behaviour, *Chaos Solitons Fractals*, **70** (2015), 58–68. https://doi.org/10.1016/j.chaos.2014.11.008

32. A. R. Ives, A. P. Dobson, Antipredator behavior and the population dynamics of simple predator-prey systems, *Am. Nat.*, **130** (1987), 431–447. https://doi.org/10.1086/284719

33. K. D. Prasad, B. S. R. V. Prasad, Qualitative analysis of additional food provided predator-prey system with anti-predator behaviour in prey, *Nonlinear Dyn.*, **96** (2019), 1765–1793. https://doi.org/10.1007/s11071-019-04883-0

34. F. Chen, On a nonlinear nonautonomous predator-prey model with diffusion and distributed delay, *J. Comput. Appl. Math.*, **180** (2005), 33–49. https://doi.org/10.1016/j.cam.2004.10.001

35. S. H. Strogatz, *Nonlinear Dynamics and Chaos with Student Solutions Manual: With Applications to Physics, Biology, Chemistry, and Engineering*, CRC Press, 2018.

36. W. M. Liu, Criterion of hopf bifurcations without using eigenvalues, *J. Math. Anal. Appl.*, **182** (1994), 250–256. https://doi.org/10.1006/jmaa.1994.1079

37. M. Haque, Ratio-dependent predator-prey models of interacting populations, *Bull. Math. Biol.*, **71** (2009), 430–452. https://doi.org/10.1007/s11538-008-9368-4

38. L. Perko, *Differential Equations and Dynamical Systems*, Springer, 2013.

39. K. A. J. White, C. A. Gilligan, Spatial heterogeneity in three species, plant-parasite-hyperparasite systems, *Phil. Trans. R. Soc. Lond. B*, **353** (1998), 543–557. https://doi.org/10.1098/rstb.1998.0226

AIMS Press

© 2026 the Author(s), licensee AIMS Press. This is an open access article distributed under the terms of the Creative Commons Attribution License (https://creativecommons.org/licenses/by/4.0)